6-28-2018

Game of Frontier Orbitals: A View on the Rational Design of Novel Charge-Transfer Materials

Maxim Vadimovich Ivanov
Marquette University

Scott A. Reid
Marquette University, scott.reid@marquette.edu

Rajendra Rathore
Marquette University, rajendra.rathore@marquette.edu

Accepted version. *Journal of Physical Chemistry Letters*, Vol. 9, No. 14 (June 28, 2018): 3978-3986.

Journal of Physical Chemistry Letters, Vol. 9, No. 14 (June 28, 2018): 3978-3986. DOI.

Game of Frontier Orbitals: A View on the Rational Design of Novel Charge-Transfer Materials

Maxim V. Ivanov
Department of Chemistry, Marquette University, Milwaukee, Wisconsin
Scott A. Reid
Department of Chemistry, Marquette University, Milwaukee, Wisconsin
Rajendra Rathore
Department of Chemistry, Marquette University, Milwaukee, Wisconsin

Abstract

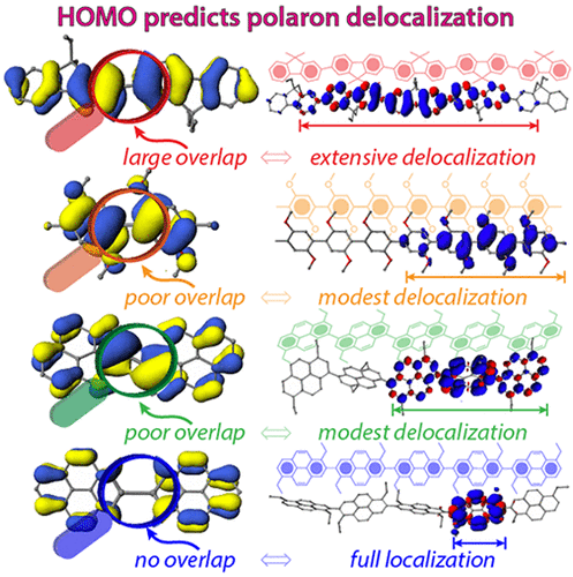

Since the first application of frontier molecular orbitals (FMOs) to rationalize stereospecificity of pericyclic reactions, FMOs have remained at the forefront of chemical theory. Yet, the practical application of FMOs in the rational design and synthesis of novel charge transfer materials remains under-appreciated. In this Perspective, we demonstrate that molecular orbital theory is a powerful and universal tool capable of rationalizing the observed redox/optoelectronic properties of various aromatic hydrocarbons in the context of their application as charge-transfer materials. Importantly, the inspection of FMOs can provide instantaneous insight into the interchromophoric electronic coupling and polaron delocalization in polychromophoric assemblies, and therefore is invaluable for the rational design and synthesis of novel materials with tailored properties.

In the realm of organic photovoltaics (OPV)(1−3) and molecular electronics(4−6) applications, the discovery of novel polycyclic aromatic hydrocarbons (PAH)(7,8) has often involved empirical synthetic approaches, but can best rely on rational design principles that lead to a material/molecule with desired electronic structure properties.(9−12) This requires a detailed intuitive understanding of the relationship between molecular and electronic structures of a candidate molecule.

A bulk heterojunction solar cell is typically formed by a blend of π-conjugated polymeric electron donors, e.g., thiophene, phenyl and/or fluorene containing molecular wires, which may also act as the light absorber, and an electron-acceptor material, e.g., fullerene.(13−16) Upon photoabsorption, the electronic excitation (i.e., exciton) travels to the donor–acceptor junction, where charge separation occurs, yielding an electrostatically bound electron and hole localized on the acceptor and donor, respectively. Although the difference in the chemical potential between the anode and cathode in an OPV device induces an appreciable electric field that favors charge separation, strong Coulombic attraction between the electron and hole at the junction often prevents long-range charge separation, leading to a reduced device quantum efficiency.(17,18) Recent studies have shown that among various factors,(19−21) efficient charge delocalization is the key for efficient long-range separation of the electron–hole pair into free carriers.(22−24) In particular, efficient delocalization of the hole on the π-conjugated polymeric donor could be the dominant factor of efficient charge separation that minimizes charge recombination.(25) Furthermore, spatially delocalized charges are often associated with high charge mobilities, which are essential for the efficient performance of OPV devices.(26,27) Unfortunately, the extent of hole/electron delocalization strongly depends upon the molecular scaffold of the electron donor, urging the development of a rational approach to control the extent of delocalization in the design of novel materials.

An understanding of mechanisms of charge delocalization in π-conjugated wires is not only limited to photovoltaic applications, but is also important in the field of single-molecule electronics.(28−30) As probed using various metal-wire-metal and donor-wire-acceptor systems, the charge transfer can be described by two limiting mechanisms:(31−34) direct tunneling between the electrodes (or from donor to acceptor), without residing on the wire, or involving the wire as an intermediate before reaching the destination. Depending on the extent of charge delocalization in long wires, the charge transfer may involve a series of hops, each described as a Marcus process.(35)

In order to understand the origin of the varied hole delocalization in different π-conjugated electron donors, we first consider the ionization of a single electron donor under steady state conditions in solution. Following Koopman's theorem and Franck–Condon principle, initial vertical ionization from the HOMO occurs rapidly on the time scale of nuclear motion, producing a vibrationally excited cation radical, followed by the ionization-induced structural (i.e., contraction/elongation of the bonds) and conformational reorganization on ps−μs time scale. In addition, the solvent serves as a sink of the initial vibrational excitation, and reorganizes to accommodate the relaxed solute. Effectively, alterations in the molecular structure and solvent establish a potential energy well for the cationic charge leading to a bound (self-trapped) state with the limited charge delocalization. The self-trapped charge together with the displaced atoms and reorganized solvent is often termed as a polaron. Although originally coined in recognition of the strong interaction between the electronic and nuclear degrees of freedom in the ionic solid,(36) the term polaron has been widely used in the literature to characterize the limited charge delocalization in a various classes of condensed matter as well as molecular systems.(22,37−43) In some literature, the term hole/electron delocalization is favored, which implies distribution of the charge as well as structural reorganization. Herein, we will use the terms polaron and hole/electron delocalization interchangeably.

Depending on the interplay between the electronic coupling (H_{ab}) between the repeat units of the polymer and the reorganization energy parameter (λ), the extent of polaron (i.e., hole or electron) delocalization may vary.(44−47) Electronic coupling is determined by the orbital overlap between interacting sites, and reorganization energy involves contribution from slow modes of solvent reorientation and fast bond vibrations associated with charge transfer. Following the two-state Marcus–Hush theory,(44) in the large electronic coupling limit ($2H_{ab} \geq \lambda$), the polaron is evenly delocalized between two sites (Figure 1A). As only one minimum is present on the potential energy surface (PES), the polaron delocalization mechanism can be termed "static" delocalization, or class III, according to the Robin-day classification.(48) Conversely, in the limit of small electronic coupling ($2H_{ab} < \lambda$), the charge is partially delocalized with the distribution maximum centered on one of the sites (Figure 1B). Due to the presence of two minima on the PES, the polaron can hop between two sites, hence, the term "dynamic" hopping can be used to describe the polaron distribution. When electronic coupling is nonexistent ($H_{ab} = 0$, Robin-Day class I), the polaron is fully localized on one site (Figure 1C).

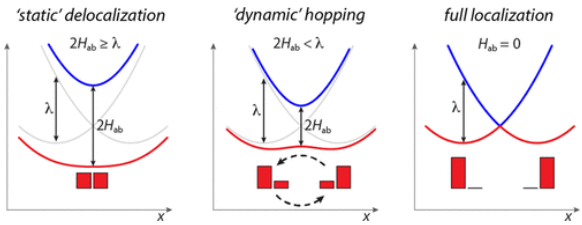

Figure 1. Three classes of polaron delocalization: static delocalization ($2H_{ab} \geq \lambda$, Robin-Day class III), dynamic hopping ($2H_{ab} < \lambda$, Robin-Day class II), and full localization ($H_{ab} = 0$, Robin-Day class I).

In the course of a rational design and synthesis of novel charge-transfer materials for photovoltaic and molecular electronics applications, one often desires to have a qualitative *a priori* understanding of the extent of polaron delocalization in the candidate material.

For example, for the purpose of promoting the long-range charge separation in the OPV device one desires a polymeric electron donor with extensive length of polaron delocalization (i.e., a wire with large H_{ab} and/or small λ). On the other hand, for molecular electronics applications, one may desire a long-range charge-transfer mechanism dominated by hole hopping, for which less delocalized polarons are required (i.e., a wire with small H_{ab} and/or large λ). While standard quantum chemistry methods such as density functional theory (DFT) allow one to accurately predict polaron delocalization in π-conjugated as well as π-stacked systems, these methods require caution, as an accurate description of the hole delocalization/stabilization is challenging for many DFT methods, in particular due to self-interaction error.(49−51)

We thus believe that models based on the Marcus–Hush and Hückel molecular orbital theories can be invaluable for the rational design of novel electron donors with the control over the hole delocalization in their cation radicals. For example, efficiency of hole delocalization in a molecular wire is largely governed by the orbital overlap between adjacent monomeric units. In order to control the orbital overlap, one often considers geometrical factors such as the interplanar dihedral angle, often referred to as simply “sterics”. It is much less recognized in the current literature that the electron density distribution of the wire plays a critically important, if not dominant, role in defining the electronic coupling.(52−55) To fill this gap, in this Perspective article we present a view on how the design of PAH-based molecular wires can be achieved by considering not only the geometrical factors but also the electron density distribution via a simple visual inspection of the frontier orbitals (FMOs) of the wire.

Organic chemists have long relied on a simple yet powerful theoretical tool to predict the stereoselectivity of pericyclic reactions.(56) Having roots in the symmetry of FMOs, here a simple visual examination of the highest occupied molecular orbital (HOMO) readily explains the stereoselectivity, as the electrocyclic reaction occurs only when like phases of the orbitals overlap to form a bond (Figure 2A).(57,58)

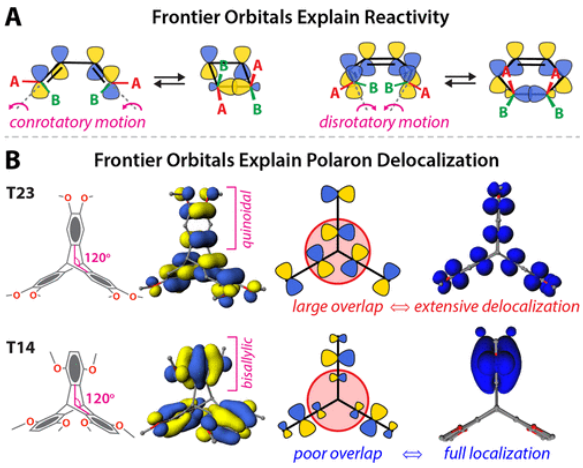

Figure 2. (A) Illustration of the Woodward–Hoffmann rules with the aid of FMO analysis.(56) (B) Large orbital overlap in triptycene derivative **T23** leads to the extensive polaron delocalization, while small orbital overlap in **T14** leads to the polaron localization on a single aromatic unit.(59)

Likewise, examination of the HOMO can be used to rationalize the extent of polaron delocalization as well as the observed redox and optical properties of polycyclic aromatic electron donors. As an example, it is known that a hexamethoxy-substituted triptycene derivative (**T23)** promotes extensive polaron (i.e., hole) delocalization over all three aromatic moieties via efficient through-space orbital overlap (i.e., large electronic coupling H_{ab}, Figure 2B).(60,61) Interestingly, as supported by electrochemistry, spectroscopy, and DFT calculations, a simple modification in the position of the methoxy groups in the isomeric triptycene **T14** leads to the localization of a hole on a single aromatic moiety,(59) despite the fact that a rigid triptycene framework with interplanar angle of 120° between aromatic rings is expected to promote efficient through-space orbital overlap

and thereby extensive hole delocalization in both triptycences.(61,62) This counterintuitive result can be readily rationalized by a simple visual inspection of HOMOs of these triptycene derivatives.(59) In **T23**, the quinoidal arrangement of the HOMO lobes in the individual aromatic rings leads to a large orbital overlap at the center of triptycene and therefore to hole delocalization over all three rings. A change in the position of the methoxy group reorients the pattern of the electron density distribution of HOMO from quinoidal to bisallylic, leading to a negligible orbital overlap at the center of the triptycene framework (i.e., small electronic coupling H_{ab}) and therefore hole localization onto a single aromatic ring (Figure 2B). Following this approach of the visual inspection of HOMO, below we consider how the experimentally determined hole delocalization in molecular wires can be rationalized with the aid of MO theory.

In order to probe experimentally the extent of polaron (i.e., electron or hole) delocalization in a molecular wire, one may resort to an oligomer approach,(63−65) where the redox and optical properties of a series of oligomers with varied number of repeat units are recorded and analyzed. For example, to probe the hole delocalization in poly-*p*-phenylenes (**PP**$_n$), a series of long soluble fluorene-based poly-*p*-phenylenes (**FPP**$_n$) with up to 16 *p*-phenylene units has been synthesized.(66) The frontier molecular orbitals (FMOs) of **FPP**$_n$ can be represented as a linear combination of the FMO of their monomeric *p*-phenylenes, with the electronic couplings alternating due to alteration in interplanar dihedral angle (Figure 3A). According to the Hückel molecular orbital theory, the HOMO and LUMO of **FPP**$_n$ are delocalized over the entire wire, while the energies (ν) of HOMO to LUMO transition evolve as cos[π/(*n*+1)] up to polymeric limit (Figure 3B).(66) The large slope in the linear trend line of the ν-vs-cos[π/(*n*+1)] plot reflects the strong interchromophoric electronic coupling and arises due to the efficient orbital overlap between adjacent *p*-phenylenes (Figure 3C).

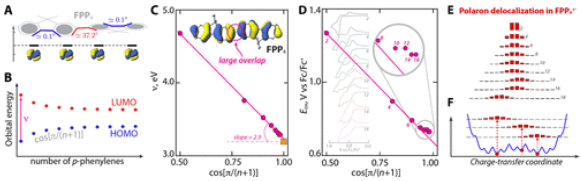

Figure 3. (A) Molecular orbital diagram of **FPP**$_4$. (B) Evolution of the HOMO and LUMO energies with varied number of *p*-phenylenes. (C) Experimental absorption energies of HOMO → LUMO transition in **FPP**$_n$ against cos[π/(*n*+1)]. The orange square corresponds to the value for polymeric **FPP**$_{108}$.(67) The HOMO of **FPP**$_4$ is shown as an example. (D) Oxidation potentials of **FPP**$_n$ against cos[π/(*n*+1)]. Cyclic voltammograms of **FPP**$_n$ are shown in the background. (E) Per-unit bar-plot representation of the polaron delocalization **FPP**$_n^{+\bullet}$ calculated using benchmarked(68−70) B1LYP40/6-31G(d) level of theory. (F) Potential energy surface of **FPP**$_{18}^{+\bullet}$ obtained from the MSM. Original data is taken from ref (66).

By contrast, oxidation potentials (E_{ox}) of **FPP**$_n$ follow a linear cos[π/(*n*+1)] trend only up to 8 *p*-phenylenes and then saturate (Figure 3D), indicating that polaron delocalization is limited to 8 *p*-phenylenes units. Indeed, natural population analysis (NPA)(71) of the electron density in **FPP**$_n^{+\bullet}$ and analysis of the oxidation-induced structural reorganization obtained from the benchmarked(68−70) B1LYP40/6-31G(d) method showed that the spin/charge/structural reorganization distributions in the ground state of **FPP**$_n^{+\bullet}$ is limited to 8 *p*-phenylenes (Figure 3E).(66) Extension of the two-state Marcus–Hush model to multiple *p*-phenylenes using a multistate Marcus model or MSM(68,72) showed that for a sufficiently long wire there are multiple quasi-isoenergetic local minima separated by ∼10 meV activation barriers (Figure 3F). It has been recently shown that the presence of such *electronic* isomers can play an important role in the charge transport in long molecular wires via both polaron tunneling and hopping mechanisms.(73−76)

Given that the polaron delocalization in **FPP**$_n$ is limited to 8 p-phenylenes, can one develop a rational approach to the design of molecular wires with a control over the extent of hole delocalization?

The example of methoxy-substituted triptycenes in Figure 2B clearly shows that the position of the electron-rich methoxy groups impacts the pattern of the electron density distribution of HOMO, giving precise control over the interchromophoric orbital overlap and electronic coupling. By the same token, incorporation of methoxy groups at 2 and 5 positions in the virgin poly-*p*-phenylene wire (i.e., poly-*p*-hydroquinone ether, **PHE**$_n$)(77,78) changes the nodal structure of HOMO from a longitudinal to transverse arrangement,(79) while also increasing the interplanar dihedral angle, leading to a reduced orbital overlap and thus reduced electronic coupling as evident from the reduced HOMO/HOMO–1 energy gap (Figure 4A). Such an alteration in the electron density distribution has a profound impact on the redox properties of the wire, which become invariant with increasing length—a feature in sharp contrast with the strong wire-length dependence of the properties in unsubstituted poly-*p*-phenylenes such as **PP**$_n$ and **FPP**$_n$ (Figure 4B).(79) Application of the MSM model in combination with benchmarked DFT calculations further revealed that polaron delocalization in **PHE**$_n^{+\bullet}$ is limited to only 3–4 units (Figure 4C), in striking contrast to the delocalization over 8 *p*-phenylenes observed in **PP**$_n^{+\bullet}$ and **FPP**$_n^{+\bullet}$. Furthermore, multiple quasi-isoenergetic local minimum structures of long **PHE**$_n^{+\bullet}$ ($n > 4$) exist with different positions of the polaron-bearing units along the wire, and a small (20 meV) interconversion barrier (Figure 4D). These isoenergetic wires can be useful to study the incoherent hopping charge-transfer in donor-wire-acceptor systems with long bridging wires due to the length-independence of the energies of the electronic states of the bridge.(80)

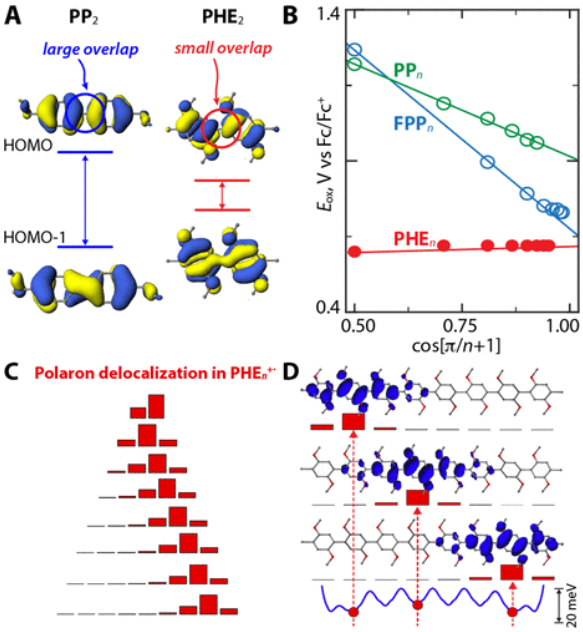

Figure 4. (A) Molecular orbital diagrams of **PP**$_2$ and **PHE**$_2$. (B) Oxidation potentials of **PHE**$_n$ against $\cos[\pi/(n+1)]$. (C) Per-unit bar-plot representation of the polaron delocalization in **PHE**$_n^{+\bullet}$ calculated using benchmarked(68−70) B1LYP40/6-31G(d) level of theory. (D) Spin-density plots of **PHE**$_8^{+\bullet}$ isomers from DFT superimposed with bar-plot representation of the hole distributions along the potential energy surface obtained from the MSM. Original data is taken from ref (79).

Considering that saturation of the redox properties and finite polaron delocalization seem to be inevitable, one may try to extend the physical length of polaron delocalization by designing wires with a larger chromophore size, as shown in Figure 5 for a case of phenylene, fluorene, hexabenzocoronene (**HBC**), and a novel **HBC**-fluorene hybrid(81) (***F*HBC**). In fact, such a strategy has been explored with wires derived from porphyrins, where the extent of charge/energy delocalization typically exceeds that observed in poly-*p*-phenylenes, in part due to their smaller reorganization energy parameter.(82−84)

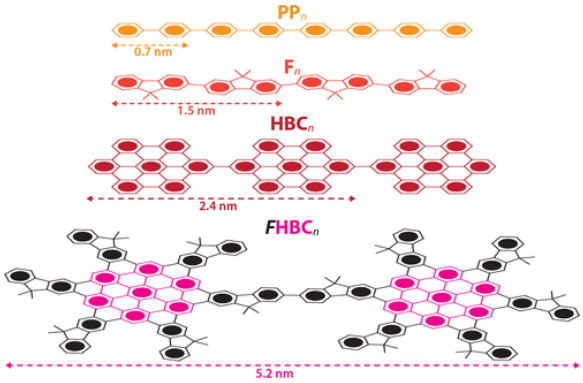

Figure 5. Examples of molecular wires with varied chromophore size.

Remarkably, a systematic variation of the chromophore size from one to three aromatic rings in a series of biaryls, i.e., biphenyl (**PP**$_2$), fluorene (**F**$_2$), bitriphenylene (**TP**$_2$), has demonstrated that hole stabilization (i.e., the difference between oxidation potentials $\Delta E_{ox} = E_{ox}$[aryl] – E_{ox}[biaryl]) *decreases* with increasing chromophore size, signifying a decrease in electronic coupling.(85) Furthermore, in the extreme case of the **HBC**-based biphenyl (**HBC**$_2$, aka "superbiphenyl")(86) with seven aromatic rings per chromophore, the hole stabilization is nearly inhibited, as the steady-state electronic absorption spectrum of **HBC**$_2^{+\bullet}$ is nearly identical to that of **HBC**$^{+\bullet}$, suggesting that in **HBC**$_2^{+\bullet}$ the hole resides on a single chromophore.(85)

This initially surprising observation is readily rationalized when one examines the electron density distribution of the HOMO in these biaryls. As the size of the chromophore increases, a total of two electrons per HOMO, in each case, spreads over a larger number of atoms, thereby decreasing the electron density at the central carbon atoms that mediate the electronic coupling through the biaryl linkage (Figure 6). As such, a doubling of the chromophore size from a single phenylene to fluorene reduces the electronic coupling nearly by half, while further expansion of the chromophore to 7 aromatic rings, as in **HBC**$_2$, reduces the coupling to a negligible value (Figure 6).

Figure 6

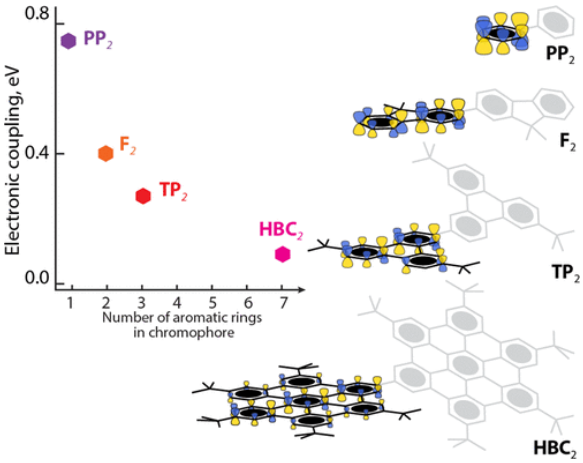

Figure 6. Left: Plot of electronic coupling against the number of aromatic rings in the chromophore. Right: Schematic illustration of the HOMOs of the biaryls illustrating the spread of the electron density as the chromophore size increases. Atomic orbitals of only one chromophore are shown for clarity.

While a small dihedral angle promotes a larger orbital overlap and electronic coupling, the amount of the available electron density at the coupling-mediating atoms is of primary importance. Thus, despite nearly identical equilibrium interplanar angles in biphenyl **PP**$_2$ and superbiphenyl **HBC**$_2$, the mechanisms of hole delocalization in their cation radicals are vastly different. One may envision that poly-**HBC**-(87,88) or ***F*HBC**-based

wires (Figure 5) would belong to a class of isoenergetic wires where redox and optoelectronic properties are length-invariant and could be interesting candidates to probe long-range charge transfer.(31,80)

The studies described thus far have demonstrated that poly fluorene wires are characterized by a strong interchromophoric electronic coupling, due to the favorable arrangement of the HOMO lobes and relatively small interplanar angle. One may expect that a structurally similar pyrene can also be considered as a candidate for the design of novel molecular wires, especially in the light of its rich electronic and optical properties (Figure 7A).(89) Surprisingly, while linking a pair of fluorenes leads to efficient (ΔE_{ox} = 370 mV) hole stabilization, linking a pair of pyrenes at the same (*para*) positions leads to a negligible (ΔE_{ox} = 10 mV) hole stabilization, despite nearly identical interplanar dihedral angles (Figure 7A).(90) This has been demonstrated using a combination of electrochemistry, spectroscopy and benchmarked DFT calculations.(90) Even more surprising, the isomeric *meta*-bipyrene (*m*-**Py**$_2$) displays an appreciable (ΔE_{ox} = 70 mV) stabilization despite a much larger interplanar dihedral angle than found in *p*-**Py**$_2$ (Figure 7A).(90)

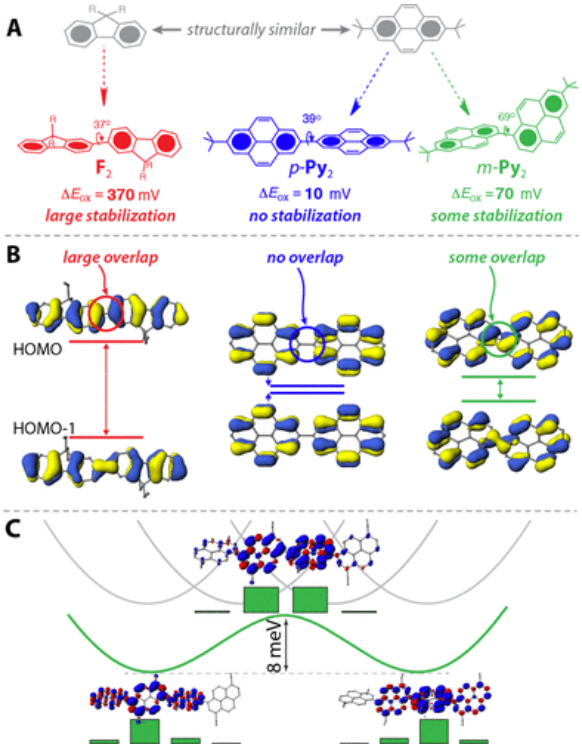

Figure 7. (A) Structures and hole stabilization (i.e., $\Delta E_{ox} = E_{ox}$[aryl] – E_{ox}[biaryl]) of **F**$_2$, *p*-**Py**$_2$ and *m*-**Py**$_2$. (B) Molecular orbital diagrams of **F**$_2$, *p*-**Py**$_2$, and *m*-**Py**$_2$. Varied HOMO/HOMO–1 energy gap reflects varied electronic coupling. (C) Potential energy surface of *m*-**Py**$_4^{+\bullet}$ obtained from MSM and spin-densities of two isomers and the transition state of *m*-**Py**$_4^{+\bullet}$ obtained using benchmarked(68–70) B1LYP40/6-31G(d) method. Original data is taken from ref (90).

Such a disparate hole stabilization between isomeric bipyrenes and bifluorene can be qualitatively rationalized by an examination of the nodal arrangement of their HOMOs and the magnitudes of the HOMO/HOMO–1 energy gaps (Figure 7B). *The HOMO of pyrene is entirely different from that of fluorene and has no HOMO electron density at the para positions!* By contrast, the availability of electron density at the *meta* position affords an appreciable overlap, despite the unfavorable dihedral angle. As a result of a small yet significant orbital overlap, hole delocalization in poly-*meta*-pyrene (*m*-**Py**$_n^{+\bullet}$) wires extends to three pyrene units, only two aromatic rings units less than in the much more strongly coupled poly-*para*-fluorene (**F**$_n^{+\bullet}$) wires. Thus, in *m*-**Py**$_4^{+\bullet}$ the steady-state polaron delocalization along the poly pyrene chain occurs by a dynamic hopping mechanism, with a relatively small interconversion barrier of 8 meV (Figure 7C), providing a conduit for long-range charge transport in longer poly pyrene wires.

It is important to bear in mind that the efficiency of the charge delocalization in the OPV devices is governed by not only the *intra*molecular delocalization through the backbone of the polymeric electron donors but also by the *inter*molecular (through-space) delocalization between adjacent π-stacked aromatic donors.(91,92) Thus, the extent of polaron delocalization studied in the isolated molecules in the examples above may change when these molecules are considered in the solid phase. In this context, the case of pillarene(93,94)—a cyclic array of five *p*-hydroquinone ethers separated by methylene linkers—is highly illustrative.(95) Hole delocalization in a single pillarene cation radical in solution is limited to only one aromatic moiety due to the poor orbital overlap (Figure 8A) as evidenced from a combination of electrochemical, spectroscopic analysis as well as DFT calculations.(95) Remarkably, upon crystallization into a solid phase, *intra*molecular hole delocalization observed in solution is diminished in favor of the formation of three *inter*molecular dimeric contacts with sandwich-like arrangement and extensive *inter/intra*molecular delocalization as judged by the analysis of the precise X-ray crystal structures of pillarene cation radical (Figure 8B). Thus, considerations of both *intra*- and *inter*molecular orbital overlaps during the rational design of novel polymeric donors provide an additional leverage for the control of their electronic structure.

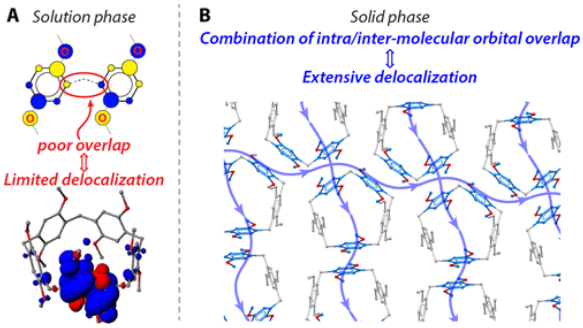

Figure 8. (A) In solution phase, hole delocalization in pillarene cation radical is limited to one aromatic moiety. (B) In solid phase, three *inter*molecular dimeric contacts formed that promote extensive *inter/intra*molecular hole delocalization.

It has been widely recognized that the geometrical factors such as the interplanar dihedral angle between adjacent units is an important factor in establishing efficient orbital overlap and thereby electronic coupling. In this Perspective we have shown that electron density distribution in the wire plays a critical if not dominant role in establishing the efficient orbital overlap. In the context of the design of novel molecular wires, the control over the orbital overlap can be achieved via changes in (1) nodal arrangement of HOMO using substituents, (2) chromophore size, (3) type of the interchromophoric linkage, and (4) the interplay between through-bond and through-space interactions.

Importantly, information on the electron density distribution can be obtained by a simple visual inspection of the HOMO and thus provide an important *qualitative* information about the electronic coupling and extent of polaron delocalization in a variety of aromatic hydrocarbons. Availability of the graphical user interfaces to various electronic structure codes provides every chemist with an immediate access to HOMO plots and can be easily incorporated in the workflow of the design and synthesis of new compounds. Since the FMOs of neutral (closed-shell) molecules are needed, there are no stringent requirements to the choice of theory level, and "default" methods (e.g., B3LYP/6-31G*) may be applicable in many cases.

> A visual inspection of the HOMO electron density distribution provides important qualitative information about the electronic coupling and extent of polaron delocalization in a variety of aromatic hydrocarbons.

In fact, for the past several years, the synthetic efforts in our research group were guided by the inspection of the nodal arrangement of HOMO of a candidate molecule and provided us with a *qualitative* prediction of its

redox/optical properties that were later confirmed experimentally.(59,90,96,97) This approach is highly familiar to every chemist, as it allows by the similar virtue the prediction of chemical reactivity and regio- and stereoselectivity of a variety of organic transformations. A simple visual inspection of HOMOs does not supersede any quantitative assessment of the hole delocalization using experimental data and benchmarked DFT methods, yet we strongly believe that such an intuitive approach can serve as an important addition to a toolkit of organic, material, and physical chemists working on the rational design and synthesis of novel materials with enhanced properties.

Acknowledgments

We thank the NSF (CHE-1508677) and NIH (R01-HL112639-04) for financial support and Professor Marat R. Talipov (New Mexico State University) for helpful discussions.

References

1 Goldschmidt, J. C.; Fischer, S. Upconversion for Photovoltaics--a Review of Materials, Devices and Concepts for Performance Enhancement. *Adv. Opt. Mater.* 2015, *3*, 510– 535, DOI: 10.1002/adom.201500024

2 Holliday, S.; Li, Y.; Luscombe, C. K. Recent Advances in High Performance Donor-acceptor Polymers for Organic Photovoltaics. *Prog. Polym. Sci.* 2017, *70*, 34– 51, DOI: 10.1016/j.progpolymsci.2017.03.003

3 Facchetti, A. Π-conjugated Polymers for Organic Electronics and Photovoltaic Cell Applications. *Chem. Mater.* 2011, *23*, 733– 758, DOI: 10.1021/cm102419z

4 Ratner, M. A Brief History of Molecular Electronics. *Nat. Nanotechnol.* 2013, *8*, 378– 381, DOI: 10.1038/nnano.2013.110

5 Heath, J. R. Molecular Electronics. *Annu. Rev. Mater. Res.* 2009, *39*, 1– 23, DOI: 10.1146/annurev-matsci-082908-145401

6 Tour, J. M. Molecular Electronics. Synthesis and Testing of Components. *Acc. Chem. Res.* 2000, *33*, 791– 804, DOI: 10.1021/ar0000612

7 Li, C.; Liu, M.; Pschirer, N. G.; Baumgarten, M.; Müllen, K. Polyphenylene-based Materials for Organic Photovoltaics. *Chem. Rev.* 2010, *110*, 6817– 6855, DOI: 10.1021/cr100052z

8 Roncali, J.; Leriche, P.; Blanchard, P. Molecular Materials for Organic Photovoltaics: Small Is Beautiful. *Adv. Mater.* 2014, *26*, 3821– 3838, DOI: 10.1002/adma.201305999

9 Allcock, H. R. Rational Design and Synthesis of New Polymeric Material. *Science* 1992, *255*, 1106– 1112, DOI: 10.1126/science.255.5048.1106

10 Farha, O. K.; Hupp, J. T. Rational Design, Synthesis, Purification, and Activation of Metal-organic Framework Materials. *Acc. Chem. Res.* 2010, *43*, 1166– 1175, DOI: 10.1021/ar1000617

11 Nijamudheen, A.; Akimov, A. V. Criticality of Symmetry in Rational Design of Chalcogenide Perovskites. *J. Phys. Chem. Lett.* 2018, *9*, 248– 257, DOI: 10.1021/acs.jpclett.7b02589

12 Imamura, Y.; Tashiro, M.; Katouda, M.; Hada, M. Automatic High-Throughput Screening Scheme for Organic Photovoltaics: Estimating the Orbital Energies of Polymers From Oligomers and Evaluating the Photovoltaic Characteristics. *J. Phys. Chem. C* 2017, *121*, 28275– 28286, DOI: 10.1021/acs.jpcc.7b08446

13 Heeger, A. J. 25th Anniversary Article: Bulk Heterojunction Solar Cells: Understanding the Mechanism of Operation. *Adv. Mater.* 2014, *26*, 10– 27, DOI: 10.1002/adma.201304373

14 Lin, Y.; Zhan, X. Oligomer Molecules for Efficient Organic Photovoltaics. *Acc. Chem. Res.* 2016, *49*, 175– 183, DOI: 10.1021/acs.accounts.5b00363

15 Mehmood, U.; Al-Ahmed, A.; Hussein, I. A. Review on Recent Advances in Polythiophene Based Photovoltaic Devices. *Renewable Sustainable Energy Rev.* 2016, *57*, 550– 561, DOI: 10.1016/j.rser.2015.12.177

16 Ross, R. B.; Cardona, C. M.; Guldi, D. M.; Sankaranarayanan, S. G.; Reese, M. O.; Kopidakis, N.; Peet, J.; Walker, B.; Bazan, G. C.; Van Keuren, E.Endohedral Fullerenes for Organic Photovoltaic Devices. *Nat. Mater.* 2009, *8*, 208– 212, DOI: 10.1038/nmat2379

17 Yuan, Y.; Reece, T. J.; Sharma, P.; Poddar, S.; Ducharme, S.; Gruverman, A.; Yang, Y.; Huang, J. Efficiency Enhancement in Organic Solar Cells with Ferroelectric Polymers. *Nat. Mater.* 2011, *10*, 296, DOI: 10.1038/nmat2951

18 Deibel, C.; Strobel, T.; Dyakonov, V. Role of the Charge Transfer State in Organic Donor--acceptor Solar Cells. *Adv. Mater.* 2010, *22*, 4097– 4111, DOI: 10.1002/adma.201000376

19 Clarke, T. M.; Durrant, J. R. Charge Photogeneration in Organic Solar Cells. *Chem. Rev.* 2010, *110*, 6736– 6767, DOI: 10.1021/cr900271s

20 Candiotto, G.; Torres, A.; Mazon, K. T.; Rego, L. G. Charge Generation in Organic Solar Cells: Interplay of Quantum Dynamics, Decoherence, and Recombination. *J. Phys. Chem. C* 2017, *121*, 23276– 23286, DOI: 10.1021/acs.jpcc.7b07165

21 McMahon, D. P.; Cheung, D. L.; Troisi, A. Why Holes and Electrons Separate So Well in Polymer/fullerene Photovoltaic Cells. *J. Phys. Chem. Lett.* 2011, *2*, 2737– 2741, DOI: 10.1021/jz201325g

22 Tamura, H.; Burghardt, I. Ultrafast Charge Separation in Organic Photovoltaics Enhanced by Charge Delocalization and Vibronically Hot Exciton Dissociation. *J. Am. Chem. Soc.* 2013, *135*, 16364– 16367, DOI: 10.1021/ja4093874

23 Bakulin, A. A.; Rao, A.; Pavelyev, V. G.; van Loosdrecht, P. H. M.; Pshenichnikov, M. S.; Niedzialek, D.; Cornil, J.; Beljonne, D.; Friend, R. H. The Role of Driving Energy and Delocalized States for Charge Separation in Organic Semiconductors. *Science* 2012, *335*, 1340– 1344, DOI: 10.1126/science.1217745

24 Strobel, T.; Deibel, C.; Dyakonov, V. Role of Polaron Pair Diffusion and Surface Losses in Organic Semiconductor Devices. *Phys. Rev. Lett.* 2010, *105*, 266602, DOI: 10.1103/PhysRevLett.105.266602

25 Niklas, J.; Mardis, K. L.; Banks, B. P.; Grooms, G. M.; Sperlich, A.; Dyakonov, V.; Beaupré, S.; Leclerc, M.; Xu, T.; Yu, L.Highly-efficient Charge Separation and Polaron Delocalization in Polymer--fullerene Bulk-heterojunctions: A Comparative Multi-frequency EPR and DFT Study. *Phys. Chem. Chem. Phys.* 2013, *15*, 9562– 9574, DOI: 10.1039/c3cp51477c

26 Metzger, R. *Unimolecular and Supramolecular Electronics I*; Springer-Verlag: Berlin Heidelberg, 2012.

27 Sakanoue, T.; Sirringhaus, H. Band-like Temperature Dependence of Mobility in a Solution-processed Organic Semiconductor. *Nat. Mater.* 2010, *9*, 736, DOI: 10.1038/nmat2825

28 Aradhya, S. V.; Venkataraman, L. Single-molecule Junctions Beyond Electronic Transport. *Nat. Nanotechnol.* 2013, *8*, 399, DOI: 10.1038/nnano.2013.91

29 Lambert, C. J. Basic Concepts of Quantum Interference and Electron Transport in Single-molecule Electronics. *Chem. Soc. Rev.* 2015, *44*, 875– 888, DOI: 10.1039/C4CS00203B

30 Perrin, M. L.; Burzurí, E.; van der Zant, H. S. Single-molecule Transistors. *Chem. Soc. Rev.* 2015, *44*, 902– 919, DOI: 10.1039/C4CS00231H

31 Davis, W. B.; Svec, W. A.; Ratner, M. A.; Wasielewski, M. R. Molecular-wire Behaviour in P-phenylenevinylene Oligomers. *Nature* 1998, *396*, 60– 63, DOI: 10.1038/23912

32 Gilbert, M.; Albinsson, B. Photoinduced Charge and Energy Transfer in Molecular Wires. *Chem. Soc. Rev.* 2015, *44*, 845– 862, DOI: 10.1039/C4CS00221K

33 Ho Choi, S.; Kim, B.; Frisbie, C. D. Electrical Resistance of Long Conjugated Molecular Wires. *Science* 2008, *320*, 1482– 1486, DOI: 10.1126/science.1156538

34 Wenger, O. S. Photoinduced Electron and Energy Transfer in Phenylene Oligomers. *Chem. Soc. Rev.* 2011, *40*, 3538– 3550, DOI: 10.1039/c1cs15044h

35 Li, G.; Govind, N.; Ratner, M. A.; Cramer, C. J.; Gagliardi, L. Influence of Coherent Tunneling and Incoherent Hopping on the Charge Transfer Mechanism in Linear Donor-Bridge-Acceptor Systems. *J. Phys. Chem. Lett.* 2015, *6*, 4889– 4897, DOI: 10.1021/acs.jpclett.5b02154

36 Landau, L. D. On the Motion of Electrons in a Crystal Lattice. *Phys. Z. Sowjet.* 1933, *3*, 664– 665

37 Holstein, T. Studies of Polaron Motion: Part I. The Molecular-crystal Model. *Ann. Phys.* 1959, *8*, 325– 342, DOI: 10.1016/0003-4916(59)90002-8

38 Holstein, T. Studies of Polaron Motion: Part II. The “small” Polaron. *Ann. Phys.* 1959, *8*, 343– 389, DOI: 10.1016/0003-4916(59)90003-X

39 Stafström, S.; Bredas, J. L.; Epstein, A. J.; Woo, H. S.; Tanner, D. B.; Huang, W. S.; MacDiarmid, A. G. Polaron Lattice in Highly Conducting Polyaniline: Theoretical and Optical Studies. *Phys. Rev. Lett.* 1987, *59*, 1464, DOI: 10.1103/PhysRevLett.59.1464

40 Bonča, J.; Trugman, S. A.; Batistić, I. Holstein Polaron. *Phys. Rev. B: Condens. Matter Mater. Phys.* 1999, *60*, 1633, DOI: 10.1103/PhysRevB.60.1633

41 Ghosh, R.; Pochas, C. M.; Spano, F. C. Polaron Delocalization in Conjugated Polymer Films. *J. Phys. Chem. C* 2016, *120*, 11394– 11406, DOI: 10.1021/acs.jpcc.6b02917

42 Donati, G.; Lingerfelt, D. B.; Petrone, A.; Rega, N.; Li, X. "Watching" Polaron Pair Formation From First-Principles Electron-Nuclear Dynamics. *J. Phys. Chem. A* 2016, *120*, 7255– 7261, DOI: 10.1021/acs.jpca.6b06419

43 Neukirch, A. J.; Nie, W.; Blancon, J.-C.; Appavoo, K.; Tsai, H.; Sfeir, M. Y.; Katan, C.; Pedesseau, L.; Even, J.; Crochet, J. J.Polaron Stabilization by Cooperative Lattice Distortion and Cation Rotations in Hybrid Perovskite Materials. *Nano Lett.* 2016, *16*, 3809– 3816, DOI: 10.1021/acs.nanolett.6b01218

44 Brunschwig, B. S.; Creutz, C.; Sutin, N. Optical Transitions of Symmetrical Mixed-valence Systems in the Class II--III Transition Regime. *Chem. Soc. Rev.* 2002, *31*, 168– 184, DOI: 10.1039/b008034i

45 Heckmann, A.; Lambert, C. Organic Mixed-Valence Compounds: A Playground for Electrons and Holes. *Angew. Chem., Int. Ed.* 2012, *51*, 326– 392, DOI: 10.1002/anie.201100944

46 Kaupp, M.; Renz, M.; Parthey, M.; Stolte, M.; Würthner, F.; Lambert, C. Computational and Spectroscopic Studies of Organic Mixed-valence Compounds: Where Is the Charge?. *Phys. Chem. Chem. Phys.* 2011, *13*, 16973– 16986, DOI: 10.1039/c1cp21772k

47 Talipov, M. R.; Navale, T. S.; Hossain, M. M.; Shukla, R.; Ivanov, M. V.; Rathore, R. Dihedral Angle-Controlled Crossover From Static Hole Delocalization to Dynamic Hopping in Biaryl Cation Radicals. *Angew. Chem., Int. Ed.* 2017, *56*, 266– 269, DOI: 10.1002/anie.201609695

48 Robin, M. B.; Day, P. Mixed Valence Chemistry-a Survey and Classification. *Adv. Inorg. Chem. Radiochem.* 1968, *10*, 247– 422, DOI: 10.1016/S0065-2792(08)60179-X

49 Bao, J. L.; Gagliardi, L.; Truhlar, D. G. Self-Interaction Error in Density Functional Theory: An Appraisal. *J. Phys. Chem. Lett.* 2018, *9*, 2353– 2358, DOI: 10.1021/acs.jpclett.8b00242

50 Cohen, A. J.; Mori-Sánchez, P.; Yang, W. Challenges for Density Functional Theory. *Chem. Rev.* 2012, *112*, 289– 320, DOI: 10.1021/cr200107z

51 Zhang, Y.; Yang, W. A Challenge for Density Functionals: Self-interaction Error Increases for Systems with a Noninteger Number of Electrons. *J. Chem. Phys.* 1998, *109*, 2604– 2608, DOI: 10.1063/1.476859

52 Beljonne, D.; Pourtois, G.; Ratner, M. A.; Brédas, J. L. Pathways for Photoinduced Charge Separation in DNA Hairpins. *J. Am. Chem. Soc.* 2003, *125*, 14510– 14517, DOI: 10.1021/ja035596f

53 Neuteboom, E. E.; Meskers, S. C. J.; van Hal, P. A.; van Duren, J. K. J.; Meijer, E. W.; Janssen, R. A. J.; Dupin, H.; Pourtois, G.; Cornil, J.; Lazzaroni, R.Alternating Oligo(p-phenylene Vinylene)--perylene Bisimide Copolymers: Synthesis, Photophysics, and Photovoltaic Properties of a New Class of Donor--acceptor Materials. *J. Am. Chem. Soc.* 2003, *125*, 8625– 8638, DOI: 10.1021/ja034926t

54 Merz, J.; Fink, J.; Friedrich, A.; Krummenacher, I.; Al Mamari, H.; Lorenzen, S.; Hähnel, M.; Eichhorn, A.; Moos, M.; Holzapfel, M.Pyrene MO Shuffle - Controlling Excited State and Redox Properties by Changing the Nature of the Frontier Orbitals. *Chem. - Eur. J.* 2017, *23*, 13164– 13180, DOI: 10.1002/chem.201702594

55 Rodriguez-Gonzalez, S.; Xie, Z.; Galangau, O.; Selvanathan, P.; Norel, L.; Van Dyck, C.; Costuas, K.; Frisbie, C. D.; Rigaut, S.; Cornil, J. HOMO Level Pinning in Molecular Junctions: Joint Theoretical and Experimental Evidence. *J. Phys. Chem. Lett.* 2018, *9*, 2394– 2403, DOI: 10.1021/acs.jpclett.8b00575

56 Woodward, R. B.; Hoffmann, R. Stereochemistry of Electrocyclic Reactions. *J. Am. Chem. Soc.* 1965, *87*, 395– 397, DOI: 10.1021/ja01080a054

57 Hoffmann, R. A Claim on the Development of the Frontier Orbital Explanation of Electrocyclic Reactions. *Angew. Chem., Int. Ed.* 2004, *43*, 6586– 6590, DOI: 10.1002/anie.200461440

58 Geerlings, P.; Ayers, P. W.; Toro-Labbé, A.; Chattaraj, P. K.; De Proft, F. The Woodward-Hoffmann Rules Reinterpreted by Conceptual Density Functional Theory. *Acc. Chem. Res.* 2012, *45*, 683– 695, DOI: 10.1021/ar200192t

59 Talipov, M. R.; Navale, T. S.; Rathore, R. The HOMO Nodal Arrangement in Polychromophoric Molecules and Assemblies Controls the Interchromophoric Electronic Coupling. *Angew. Chem., Int. Ed.* 2015, *54*, 14468– 14472, DOI: 10.1002/anie.201506402

60 Ivanova, L. V.; Wang, D.; Lindeman, S.; Ivanov, M. V.; Rathore, R. Probing Charge Delocalization in Solid State Polychromophoric Cation Radicals Using X-ray Crystallography and DFT Calculations. *J. Phys. Chem. C* 2018, *122*, 9339– 9345, DOI: 10.1021/acs.jpcc.8b02184

61 Navale, T. S.; Thakur, K.; Vyas, V. S.; Wadumethrige, S. H.; Shukla, R.; Lindeman, S. V.; Rathore, R. Charge Delocalization in Self-assembled Mixed-valence Aromatic Cation Radicals. *Langmuir* 2012, *28*, 71– 83, DOI: 10.1021/la202611w

62 Ivanov, M. V.; Wadumethrige, S. H.; Wang, D.; Rathore, R. Through--Space or Through--Bond? The Important Role of Cofaciality in Orbital Reordering and Its Implications for Hole (De) Stabilization in Polychromophoric Assemblies. *J. Phys. Chem. C* 2017, *121*, 15639– 15643, DOI: 10.1021/acs.jpcc.7b05804

63 Müllen, K.; Wegner, G. *Electronic Materials: The Oligomer Approach*; John Wiley & Sons: Weinheim, Germany, 2008.

64 Chi, C.; Wegner, G. Chain-Length Dependence of the Electrochemical Properties of Conjugated Oligofluorenes. *Macromol. Rapid Commun.* 2005, *26*, 1532– 1537, DOI: 10.1002/marc.200500437

65 Camarada, M. B.; Jaque, P.; Díaz, F. R.; Del Valle, M. A. Oxidation Potential of Thiophene Oligomers: Theoretical and Experimental Approach. *J. Polym. Sci., Part B: Polym. Phys.* 2011, *49*, 1723– 1733, DOI: 10.1002/polb.22360

66 Ivanov, M. V.; Talipov, M. R.; Boddeda, A.; Abdelwahed, S. H.; Rathore, R. Hückel Theory+ Reorganization Energy= Marcus-Hush TheoryBreakdown of the 1/n Trend in Π-Conjugated Poly-p-phenylene Cation Radicals Is Explained. *J. Phys. Chem. C* 2017, *121*, 1552– 1561, DOI: 10.1021/acs.jpcc.6b12111

67 Klaerner, G.; Miller, R. D. Polyfluorene Derivatives: Effective Conjugation Lengths From Well-defined Oligomers. *Macromolecules* 1998, *31*, 2007– 2009, DOI: 10.1021/ma971073e

68 Talipov, M. R.; Boddeda, A.; Timerghazin, Q. K.; Rathore, R. Key Role of End-capping Groups in Optoelectronic Properties of Poly-p-phenylene Cation Radicals. *J. Phys. Chem. C* 2014, *118*, 21400– 21408, DOI: 10.1021/jp5082752

69 Ivanov, M.; Talipov, M.; Navale, T.; Rathore, R. Ask Not How Many, but Where They Are: Substituents Control Energetic Ordering of Frontier Orbitals/Electronic Structures in Isomeric Methoxy-Substituted Dibenzochrysenes. *J. Phys. Chem. C* 2018, *122*, 2539– 2545, DOI: 10.1021/acs.jpcc.7b11232

70 Kokkin, D.; Ivanov, M. V.; Loman, J.; Cai, J.-Z.; Rathore, R.; Reid, S. A. Strength of Π-Stacking, From Neutral to Cation: Precision Measurement of Binding Energies in An Isolated Π-Stacked Dimer. *J. Phys. Chem. Lett.* 2018, *9*, 2058– 2061, DOI: 10.1021/acs.jpclett.8b00742

71 Reed, A. E.; Weinstock, R. B.; Weinhold, F. Natural Population Analysis. *J. Chem. Phys.* 1985, *83*, 735– 746, DOI: 10.1063/1.449486

72 Talipov, M. R.; Ivanov, M. V.; Rathore, R. Inclusion of Asymptotic Dependence of Reorganization Energy in the Modified Marcus-Based Multistate Model Accurately Predicts Hole Distribution in Poly-p-phenylene Wires. *J. Phys. Chem. C* 2016, *120*, 6402– 6408, DOI: 10.1021/acs.jpcc.6b00514

73 Zaikowski, L.; Kaur, P.; Gelfond, C.; Selvaggio, E.; Asaoka, S.; Wu, Q.; Chen, H.-C.; Takeda, N.; Cook, A. R.; Yang, A.Polarons, Bipolarons, and Side-by-side Polarons in Reduction of Oligofluorenes. *J. Am. Chem. Soc.* 2012, *134*, 10852– 10863, DOI: 10.1021/ja301494n

74 Smith, C. E.; Odoh, S. O.; Ghosh, S.; Gagliardi, L.; Cramer, C. J.; Frisbie, C. D. Length-Dependent Nanotransport and Charge Hopping Bottlenecks in Long Thiophene-Containing Π-Conjugated Molecular Wires. *J. Am. Chem. Soc.* 2015, *137*, 15732– 15741, DOI: 10.1021/jacs.5b07400

75 Taherinia, D.; Smith, C. E.; Ghosh, S.; Odoh, S. O.; Balhorn, L.; Gagliardi, L.; Cramer, C. J.; Frisbie, C. D. Charge Transport in 4 Nm Molecular Wires with Interrupted Conjugation: Combined Experimental and Computational Evidence for Thermally Assisted Polaron Tunneling. *ACS Nano* 2016, *10*, 4372– 4383, DOI: 10.1021/acsnano.5b08126

76 Lambert, C.; Nöll, G.; Schelter, J. Bridge-mediated Hopping or Superexchange Electron-transfer Processes in Bis(triarylamine) Systems. *Nat. Mater.* 2002, *1*, 69– 73, DOI: 10.1038/nmat706

77 Walther, M. E.; Wenger, O. S. Tuning the Rates of Long-range Charge Transfer Across Phenylene Wires. *ChemPhysChem* 2009, *10*, 1203– 1206, DOI: 10.1002/cphc.200900163

78 Hanss, D.; Walther, M. E.; Wenger, O. S. Accelerated Hole Transfer Across a Molecular Double Barrier. *Chem. Commun. (Cambridge, U. K.)* 2010, *46*, 7034– 7036, DOI: 10.1039/c0cc01591a

79 Ivanov, M. V.; Chebny, V. J.; Talipov, M. R.; Rathore, R. Poly-p-hydroquinone Ethers: Isoenergetic Molecular Wires with Length-Invariant Oxidation Potentials and Cation Radical Excitation Energies. *J. Am. Chem. Soc.* 2017, *139*, 4334– 4337, DOI: 10.1021/jacs.7b01226

80 Goldsmith, R. H.; Sinks, L. E.; Kelley, R. F.; Betzen, L. J.; Liu, W.; Weiss, E. A.; Ratner, M. A.; Wasielewski, M. R. Wire-like Charge Transport at Near Constant Bridge Energy Through Fluorene Oligomers. *Proc. Natl. Acad. Sci. U. S. A.* 2005, *102*, 3540– 3545, DOI: 10.1073/pnas.0408940102

81 Navale, T. S.; Ivanov, M. V.; Hossain, M. M.; Rathore, R. FHBC, a Hexa-peri-hexabenzocoronene-Fluorene Hybrid: A Platform for Highly Soluble, Easily Functionalizable HBCs with An Expanded Graphitic Core. *Angew. Chem., Int. Ed.* 2018, *57*, 790– 794, DOI: 10.1002/anie.201711739

82 Peeks, M. D.; Tait, C. E.; Neuhaus, P.; Fischer, G. M.; Hoffmann, M.; Haver, R.; Cnossen, A.; Harmer, J. R.; Timmel, C. R.; Anderson, H. L. Electronic Delocalization in the Radical Cations of Porphyrin Oligomer Molecular Wires. *J. Am. Chem. Soc.* 2017, *139*, 10461– 10471, DOI: 10.1021/jacs.7b05386

83 Rawson, J.; Angiolillo, P. J.; Therien, M. J. Extreme Electron Polaron Spatial Delocalization in Π-conjugated Materials. *Proc. Natl. Acad. Sci. U. S. A.* 2015, *112*, 13779– 13783, DOI: 10.1073/pnas.1512318112

84 Parkinson, P.; Kondratuk, D. V.; Menelaou, C.; Gong, J. Q.; Anderson, H. L.; Herz, L. M. Chromophores in Molecular Nanorings: When Is a Ring a Ring?. *J. Phys. Chem. Lett.* 2014, *5*, 4356– 4361, DOI: 10.1021/jz5022153

85 Ivanov, M.; Wang, D.; Rathore, R. From Static to Dynamic: The Size/HOMO Density Dependence of Electronic Coupling in Model Biaryl Wires Controls the Mechanism of Hole Delocalization. *J. Am. Chem. Soc.* 2018, *140*, 4765– 4769, DOI: 10.1021/jacs.8b00466

86 Ito, S.; Herwig, P. T.; Böhme, T.; Rabe, J. P.; Rettig, W.; Müllen, K. Bishexa-p Eri-hexabenzocoronenyl: A Superbiphenyl. *J. Am. Chem. Soc.* 2000, *122*, 7698– 7706, DOI: 10.1021/ja000850e

87 Wu, J.; Watson, M. D.; Tchebotareva, N.; Wang, Z.; Müllen, K. Oligomers of Hexa-peri-hexabenzocoronenes As "super-oligophenylenes": Synthesis, Electronic Properties, and Self-assembly. *J. Org. Chem.* 2004, *69*, 8194– 8204, DOI: 10.1021/jo0490301

88 Lu, D.; Zhuang, G.; Wu, H.; Wang, S.; Yang, S.; Du, P. A Large Π-Extended Carbon Nanoring Based on Nanographene Units: Bottom-Up Synthesis, Photophysical Properties, and Selective Complexation with Fullerene C70. *Angew. Chem., Int. Ed.* 2017, *56*, 158– 162, DOI: 10.1002/anie.201608963

89 Figueira-Duarte, T. M.; Müllen, K. Pyrene-based Materials for Organic Electronics. *Chem. Rev.* 2011, *111*, 7260– 7314, DOI: 10.1021/cr100428a

90 Ivanov, M. V.; Thakur, K.; Boddeda, A.; Wang, D.; Rathore, R. Nodal Arrangement of HOMO Controls the Turning On/Off the Electronic Coupling in Isomeric Polypyrene Wires. *J. Phys. Chem. C* 2017, *121*, 9202– 9208, DOI: 10.1021/acs.jpcc.7b02264

91 Hartnett, P. E.; Timalsina, A.; Matte, H. S. S. R.; Zhou, N.; Guo, X.; Zhao, W.; Facchetti, A.; Chang, R. P. H.; Hersam, M. C.; Wasielewski, M. R.Slip-stacked Perylenediimides As An Alternative Strategy for High Efficiency Nonfullerene Acceptors in Organic Photovoltaics. *J. Am. Chem. Soc.* 2014, *136*, 16345– 16356, DOI: 10.1021/ja508814z

92 Batra, A.; Kladnik, G.; Vázquez, H.; Meisner, J. S.; Floreano, L.; Nuckolls, C.; Cvetko, D.; Morgante, A.; Venkataraman, L. Quantifying Through-space Charge Transfer Dynamics in Π-coupled Molecular Systems. *Nat. Commun.* 2012, *3*, 1086, DOI: 10.1038/ncomms2083

93 Ogoshi, T.; Kanai, S.; Fujinami, S.; Yamagishi, T.-A.; Nakamoto, Y. Para-Bridged Symmetrical Pillar[5]arenes: Their Lewis Acid Catalyzed Synthesis and Host-guest Property. *J. Am. Chem. Soc.* 2008, *130*, 5022– 5023, DOI: 10.1021/ja711260m

94 Rathore, R.; Kochi, J. K. Radical-Cation Catalysis in the Synthesis of Diphenylmethanes Via the Dealkylative Coupling of Benzylic Ethers. *J. Org. Chem.* 1995, *60*, 7479– 7490, DOI: 10.1021/jo00128a020

95 Ivanov, M.; Wang, D.; Navale, T.; Lindeman, S.; Rathore, R. From Intramolecular (Circular) in An Isolated Molecule to Intermolecular Hole Delocalization in a Two-Dimensional Solid-State Assembly: The Case of Pillarene. *Angew. Chem., Int. Ed.* 2018, *57*, 2144– 2149, DOI: 10.1002/anie.201712159

96 Ivanov, M. V.; Wang, D.; Rathore, R. From Static to Dynamic: Electron Density of HOMO at Biaryl Linkage Controls the Mechanism of Hole Delocalization. *J. Am. Chem. Soc.* 2018, *140*, 4765– 4769, DOI: 10.1021/jacs.8b00466

97 Ivanova, L. V.; Navale, T. S.; Wang, D.; Lindeman, S.; Ivanov, M. V.; Rathore, R. Towards the Rational Design of Novel Charge-transfer Materials: Biaryls with a Dihedral Angle-independent Hole Delocalization Mechanism. *Chem. Commun. (Cambridge, U. K.)* 2018, *54*, 5851, DOI: 10.1039/C8CC02595A